Structure determination of Ag(111)($\sqrt{3}\times\sqrt{3}$)$R30°$-Sb by low-energy electron diffraction

E. A. Soares*
Departamento de Física, ICEx-UFMG, CP 702, Belo Horizonte, MG, Brasil-CEP 30123-970

C. Bittencourt
Department of Physics, University of Warwick, Coventry CV4 7AL, United Kingdom

V. B. Nascimento and V. E. de Carvalho
Departamento de Física, ICEx-UFMG, CP 702, Belo Horizonte, MG, Brasil-CEP 30123-970

C. M. C. de Castilho
Instituto de Física-UFBA, Salvador, BA, Brasil-CEP 40210-340

C. F. McConville
Department of Physics, University of Warwick, Coventry CV4 7AL, United Kingdom

A. V. de Carvalho
Departamento de Física, ICEx-UFMG, CP 702, Belo Horizonte, MG, Brasil-CEP 30123-970

D. P. Woodruff
Department of Physics, University of Warwick, Coventry CV4 7AL, United Kingdom
(Received 28 October 1999)

A quantitative structure determination of the Ag(111)($\sqrt{3}\times\sqrt{3}$)$R30°$-Sb surface has been performed using low energy electron diffraction. Six possible structural models were tested: Sb overlayers with four different adsorption sites and a substitutional alloy surface layer, with or without a stacking fault relative to the underlying substrate. The results clearly favor the faulted alloy surface model with all outermost layer Sb and Ag atoms occupying hcp hollow sites, in agreement with a recent x-ray diffraction study of this surface phase and both x-ray diffraction and medium energy ion scattering studies of the related Cu(111)($\sqrt{3}\times\sqrt{3}$)$R30°$-Sb surface.

I. INTRODUCTION

A detailed understanding of the mechanisms involved in the epitaxial growth of metals is of both fundamental interest and technological importance. For the growth of novel magnetic film structures or multilayer films for x-ray mirrors, good control of the interface structure and surface flatness is important to obtain the best material properties. Both interfacial strain and surface free energy contribute to the criteria that determine whether a film undergoes layer-by-layer growth (Frank–Van der Merwe), islanding (Volmer-Weber), or layer-by-layer growth followed by islanding (Stranski-Krastanov). It has been shown that the introduction of a surfactant (a suitable adsorbate that remains at the free surface during growth) alters the surface free energy and can thus change the growth mode of a film. This has led to surfactant mediated epitaxy being used to achieve layer-by-layer growth in both metal and semiconductor systems.[1–6]

One problem of particular interest is the role of submonolayer quantities of Sb as a surfactant in the homoepitaxial growth of metals, mainly Ag on Ag(111).[6,7] The Sb atoms appear to constantly diffuse or segregate to the growing surface, effectively ''floating'' on top of the surface during epitaxy and continuing to act as a surfactant throughout the growth process. A knowledge of the structural and electronic properties of the growing surface, as well as the mechanism of interaction between surfactant and the surface atoms, is necessary for a complete understanding of this process. Structural characterization of the Sb/Ag(111) system has been performed by Noakes *et al.*[8] In that study, the overlayer structures formed by adsorption of Sb on Ag(111) were studied using coaxial impact collision ion scattering spectroscopy (CAICISS) together with qualitative low energy electron diffraction (LEED). At Sb coverages up to several atomic layers there was evidence of layer-by-layer growth at room temperature, although the individual layers showed no long-range order. Subsequent annealing gave rise to two ordered phases, ($\sqrt{3}\times\sqrt{3}$)$R30°$-Sb and ($2\sqrt{3}\times 2\sqrt{3}$)$R30°$-Sb. Neon ion CAICISS data were used to distinguish between overlayer and substitutional structural models for the ($\sqrt{3}\times\sqrt{3}$)$R30°$-Sb phase and pure substitutional and mixed substitutional-overlayer models for the ($2\sqrt{3}\times 2\sqrt{3}$)$R30°$-Sb phase. Despite the complexity of the multiple scattering contributions, these data favored the substitutional adsorption site for the ($\sqrt{3}\times\sqrt{3}$)$R30°$-Sb phase. For the ($2\sqrt{3}\times 2\sqrt{3}$)$R30°$-Sb phase, the data were best described by a model involving an ordered $p(2\times 2)$-Sb overlayer superimposed on the ($\sqrt{3}\times\sqrt{3}$)$R30°$-Sb surface.

These conclusions of the CAICISS analysis are in agree-

ment with those obtained by *ab initio* calculations for Sb adsorbed on Ag(111).[9] Those calculations showed that it is energetically most favorable for the adsorbed Sb atoms to occupy substitutional sites within the top layer for coverages up to the formation of a 0.33 monolayer (ML) $(\sqrt{3}\times\sqrt{3})R30°$-Sb structure. They also showed that the substitutional Sb adsorbates occupy the surface vacancy in a position very close to the ideal (bulk-terminated) fcc location of the substituted Ag atom with an outward relaxation of only 5% to 8% of the interlayer spacing, i.e., about 0.12–0.19 Å. Scanning tunneling microscopy (STM) has also been used to study the growth of Ag on Ag(111) in the presence of preadsorbed Sb (Refs. 7,10,11); at very low Sb coverages the images show small indentations, attributed to individual Sb atoms in substitutional sites within the first layer. STM was also used to study in more detail the difference between as-deposited and annealed Sb precovered surfaces on the growth of the first monolayer of Ag on Ag(111).[11] At somewhat higher coverages, the surface showed ordered islands both on top of the surface and at step edges with a $(\sqrt{3}\times\sqrt{3})R30°$ periodicity and random indentations attributed to substitutional sites in the surface. The main focus of those STM studies was an attempt to understand the mechanism whereby Sb atoms ''float'' to the surface as the Ag films grow, but they also provide evidence that Sb atoms occupy substitutional sites at low coverage.

Here, our concern is to establish, in a quantitative fashion, the structure of the ordered Ag(111)$(\sqrt{3}\times\sqrt{3})R30°$-Sb phase. In this context the most relevant recent work is a surface x-ray diffraction (SXRD) study of this phase.[12] The conclusion of that investigation was that, although the Sb atoms do substitute for 0.33 ML of Ag atoms in the outermost layer to form a surface alloy, consistent with the results of the previous theory and experimental CAICISS studies, all the Ag and Sb atoms in this top layer occupied hcp hollow sites (above second layer Ag atoms). In effect, therefore, there is a stacking fault at the surface alloy/substrate interface. That investigation also included a similar structural study of the Cu(111)$(\sqrt{3}\times\sqrt{3})R30°$-Sb phase, for which the same faulted alloy surface structure was found. Very recently this result for the Cu(111) surface has been confirmed in a medium energy ion scattering investigation.[13] Curiously, an independent SXRD study of this phase[14] concluded that the structure comprised an unfaulted surface alloy, but the possibility of a faulted surface alloy was not considered in the analysis in that work.

In this paper we present a quantitative LEED study of the Ag(111)$(\sqrt{3}\times\sqrt{3})R30°$-Sb surface structure using multiple scattering simulations and an objective reliability factor (R factor) to aid experiment-theory comparison. A range of possible surface structural models have been tested including both overlayer and substitutional phases, and, in particular, this stacking fault alloy model.

II. EXPERIMENTAL DETAILS

The experiments were conducted using a standard ultrahigh vacuum chamber equipped with a range of facilities for sample preparation and surface characterization together with a computer-controlled LEED diffractometer in the Physics Department of the University of Warwick. The base pressure of the chamber was typically $(1-2)\times10^{-10}$ torr. The Ag(111) crystal slice was cut by spark erosion from a crystal oriented by Laue x-ray diffraction. The surface was then polished using progressively finer grades of diamond paste to produce a mirror finish. After insertion into vacuum, the sample was cleaned using cycles of sputtering (Ar^+ ions with 3 keV) and annealing (500 °C for 10 min). The temperature was monitored using a Chromel-Alumel thermocouple in contact with the sample. The cleaning cycles were repeated until no carbon, oxygen, or sulfur were detectable using x-ray photoelectron spectroscopy (XPS) and the LEED indicated a sharp (1×1) pattern. Deposition of a nominal 0.33 ML of Sb was carried out using a small Knudsen cell loaded with 99.9999% pure Sb and operated at a temperature of 455 °C. XPS was used to monitor the composition change at the surface. During deposition the sample was kept at room temperature, but was then subsequently annealed at a temperature of 200 °C to produce the desired $(\sqrt{3}\times\sqrt{3})R30°$ LEED pattern. Quantitative LEED intensities were recorded from 30 eV up to 370 eV at a sample temperature of 163 K (to reduce the effect of thermal vibrations) using an Omicron video-LEED system at nominal normal incidence. The intensity-voltage $[I(V)]$ curves for seven fractional-order beams $[(\frac{1}{3},\frac{1}{3}),(\frac{2}{3},\frac{1}{3}),(\frac{1}{3},\frac{2}{3}),(\frac{2}{3},\frac{1}{3}),(\frac{1}{3},\frac{2}{3}),(\frac{4}{3},\frac{2}{3}),(\frac{2}{3},\frac{4}{3})]$ and nine integal-order beams $[(0,1),(1,0),(1,\bar{1}),(0,\bar{1}),(\bar{1},0),(\bar{1},2),(1,1),(1,\bar{2}),(\bar{1},\bar{1})]$ were then extracted from the digitized LEED patterns and smoothed using a five-point least-squares cubic polynomial algorithm. The symmetry-equivalent beams were then averaged, reducing the data set from sixteen beams to three symmetry-inequivalent integral-order beams $[(0,1),(1,0),(1,1)]$ and two symmetry-inequivalent fractional-order beams $[(\frac{1}{3},\frac{1}{3}),(\frac{4}{3},\frac{2}{3})]$ encompassing a total energy range of 1000 eV.

III. THEORETICAL ASPECTS

The theoretical analysis was performed assuming the muffin-tin model for the crystal. The muffin-tin potential and the phase shifts were calculated using the BARBIERI/VAN HOVE PHASE SHIFT package.[15] In particular, a self-consistent Dirac-Fock approach was used in order to compute the self-consistent atomic orbitals for each element; the muffin-tin potential was then computed following Mattheis' prescription and the relativistic phase shifts were evaluated by numerical integration of the Dirac equation.

The full dynamic LEED calculations were performed on a Pentium II 400 MHz, running Linux, using both the LEEDFIT (Refs. 16–20) and the symmetrized automated tensor LEED (SATLEED)[15,21] packages. Six different adsorption sites for Sb were considered as starting points, namely, on-top, bridge, fcc hollow and hcp hollow, fcc substitutional and hcp substitutional (this last model also involving displacement of the outermost layer Ag atoms to hcp hollow sites with respect to the underlying substrate). Strictly, the scattering phase shifts are structure dependent, so in order to investigate the importance of this effect a different set of ten phase shifts was used for each structural model. Subsequent tests revealed that these different phase shifts had no significant influence on the quality of the resulting experiment-theory agreement.

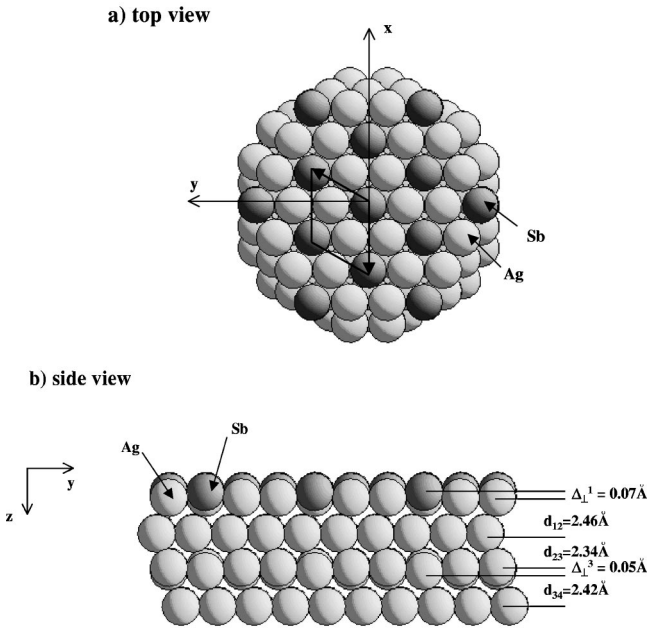

FIG. 1. The Ag(111)($\sqrt{3}\times\sqrt{3}$)$R30°$-Sb reconstructed surface. The dark spheres denote the substitutional Sb atoms, the light ones the Ag atoms. (a) Top view; (b) side view.

The experimental sample temperature (163 K) and incidence geometry (normal incidence) were assumed. For the purposes of the adjustable structural parameters the surface was considered to be formed by the three outermost layers, each layer (containing 3 atoms per surface unit mesh) being treated using the composite layer approach. All the atomic positions in these three layers were allowed to relax in the final step of the analysis, but displacements were constrained to be consistent with the point group symmetry of the substrate. The parameters varied (see also Fig. 1 and Tables I and II below) were therefore the first three interlayer distances (d_{12}, d_{23}, and d_{34}), relative displacements perpendicular to the surface (buckling) in the first and third layers ($\Delta_\perp^1$ and $\Delta_\perp^3$), and relative displacements parallel to the surface in the second layer ($\Delta_\parallel$). The bulk Debye temperature values of 200 K and 225 K were used for the Sb and Ag atoms, respectively.[22] Values of $V_0 = 10$ eV and $V_{0i} = -4$ eV were assumed for the real and imaginary parts of the inner potential, respectively, but the real part was fitted during the optimization process.

IV. RESULTS AND DISCUSSION

In the initial assessment of the six alternative structural models, the $I(V)$ curves for each one of the possible models were calculated using the LEEDFIT program over the reduced total energy range of 650 eV (40–250 eV for each spectrum). This concentration on the lower energy data enhances the sensitivity to the geometry of the outermost layer, but was also the data range used in a preliminary assessment of the system using LEED data taken at room temperature for which the higher energy range was heavily damped by the Debye-Waller factor. As a first test all Ag layer spacings were assumed to have their bulk values (2.359 Å); note that a recent LEED analysis of clean Ag(111) concluded that this surface exhibits no relaxation[23] and the Sb and Ag atoms have very similar atomic radii (1.44 Å for Sb and 1.59 Å for Ag). The resulting Pendry R factors (R_P) for each model are shown in the second column of Table I. From these values we are not able to distinguish any preferred model, and optimization of the interlayer distances for each model was clearly required. After this optimization of the first three interlayer distances, the faulted (hcp) substitutional alloy model clearly shows the lowest R_P value; the next most favorable model is the hcp overlayer, although the less probable atop overlayer has an R factor value that is only slightly larger.

Further refinement of these two most probable solutions, the faulted substitutional and hcp overlayer models, was then carried out using the full energy range (1000 eV) of the data. In this second step, the SATLEED package was used, taking the structural models obtained in the first optimization stage as the initial reference structures for the fuller optimization in which the atomic positions of all atoms of the surface layers were allowed to relax within the constraints of the point group symmetry of the substrate. For the overlayer model, no improvement in the fit was observed, whereas for the faulted substitutional model, R_P decreased from 0.45 for an energy range of 650 eV to 0.34 (with an associated vari-

TABLE II. Structural parameters for the substitutional hcp model obtained in this work and by SXRD (Ref. 12). The displacements are defined as shown in Fig. 1. The * means that the parameter was not investigated in the SXRD study but was assumed to take its bulk value.

	This work	SXRD
$\Delta_\perp^1$ (Å)	0.07 ± 0.04	0.03
$\Delta_\perp^3$ (Å)	0.05 ± 0.05	0.00*
d_{12} (Å)	2.46 ± 0.03	2.50
d_{23} (Å)	2.34 ± 0.04	2.36
d_{34} (Å)	2.42 ± 0.07	2.36*
$\Delta_\parallel$ (Å)	0.00 ± 0.07	0.06

TABLE I. R_P values for the structural models analyzed for Ag(111)($\sqrt{3}\times\sqrt{3}$)$R30°$-Sb before and after the interlayer distance optimization. The interlayer distances are the values obtained from the optimization.

Structural models	Initial R_P	Final R_P	d_{12} (Å)	d_{23} (Å)	d_{34} (Å)
faulted alloy	0.66	0.45	2.502	2.347	2.443
unfaulted alloy	0.70	0.65	2.408	2.309	2.383
overlayer hcp	0.76	0.58	2.455	2.344	2.347
overlayer fcc	0.67	0.66	2.376	2.400	2.336
overlayer top	0.69	0.59	2.454	2.415	2.365
overlayer bridge	0.81	0.78	2.359	2.359	2.359

ance of 0.06) for the extended energy range of 1000 eV. The structural parameters for this best model are presented in Table II. We can see from this table that there is an expansion of 4.3% of the first interlayer distance (d_{12}) with respect to the bulk value, a very small contraction of -0.8% of the second one (d_{23}), and an expansion of 2.6% of the third interlayer distance (d_{34}). Layer buckling was also observed in the first ($\Delta_{\perp}^{1}$) and third ($\Delta_{\perp}^{3}$) layers, the Sb atoms and the Ag atoms directly below the Sb atoms in the third layer, having a slightly different layer spacing than the surrounding Ag atoms in the same nominal layer. In the first layer, the Sb atoms move outward from the substrate whereas the Ag atoms move down toward the substrate. In the third layer the buckling is in the opposite direction, with the Ag atoms that sit ''below'' the Sb atoms moving up. Notice that in the second layer buckling of this type is symmetry forbidden. However, in this layer in-plane displacement of the atoms in the form of a contraction or expansion relative to the lateral position of the Sb atom above is possible. The recent SXRD study of this surface did find a small distortion of this type, but our results favor no such displacement ($\Delta_{\parallel}=0.00$). The structure corresponding to our best-fit solution presented in Table II is illustrated in Fig. 1.

Table II also shows the optimum structural parameter values obtained in the prior SXRD study of this surface[12] and it is clear that all values agree to within our estimated limits of precision. The largest difference in the actual optimum values of parameters investigated in both studies is in the in-plane contraction of the second layer Ag atoms around the Sb adsorbates. In particular, we find no evidence for any such distortion, while small displacements are found in the SXRD study. This difference may stem from the fact that SXRD is generally more sensitive to atom movements parallel to the surface than is LEED. On the other hand, we should note that this previous study did not consider adsorbate-induced modifications of the third Ag layer, which was assumed to be bulklike. Coupling of structural parameters is not uncommon in these surface structural methods, and it is possible that if third layer modifications were included in the SXRD analysis, this might influence the optimum value of other distortion parameters. Nevertheless, the primary conclusion to be drawn from Table II is that these two independent studies by different methods are in excellent agreement.

In particular, our results show that the hcp substitutional model, in which the surface alloy layer exhibits a stacking fault between the surface alloy layer and the underlying substrate, is clearly the favored structural model. In order to examine this more closely we have studied the variations of the R_P factor as a function of the top layer atom displacement (Δx) along the $\langle 112\rangle$ mirror plane. The displacement is defined with respect to the hcp sites, the whole surface alloy layer (one Sb atom and two Ag atoms per surface unit mesh) being displaced by the same amount. For each value of Δx, all other structural parameters were optimized in order to minimize the value of R_P. The dependence of R_P on this displacement parameter is shown in Fig. 2. The figure shows two minima in R_P. The deepest one ($R_P=0.34$) corresponds to the faulted alloy model ($\Delta x=0.0$ Å) whereas the other minimum ($R_P=0.65$) is not very well defined but corresponds to the unfaulted (fcc) alloy model ($\Delta x=1.67$ Å).

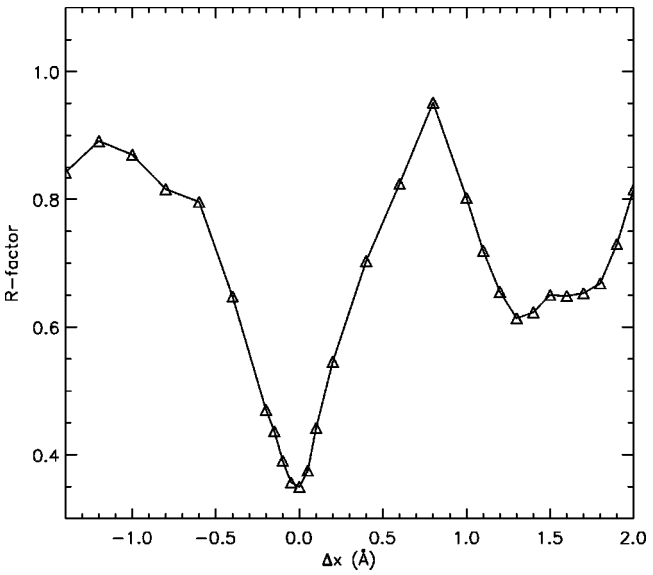

FIG. 2. The R factor R_P for a substitutional surface alloy model as a function of the magnitude of displacement of the outermost (alloy) layer parallel to the surface along a $\langle 112\rangle$ mirror plane (x axis). $\Delta x=0$ corresponds to a hcp site relative to the underlying substrate.

Figure 3 shows a comparison of the experimental $I(V)$ curves used in this study with the theoretical curves for the best-fit structural model. Clearly there is generally good agreement between the experimental and theoretical data, especially with regard to the energies of peaks, as reflected in the reasonable (but not especially low) value of the R factor.

V. CONCLUSION

From the results presented here, we are able to conclude that, of the six models of Ag(111)($\sqrt{3}\times\sqrt{3}$)$R30°$-Sb initially considered [two substitutional surface alloy structures (hcp and fcc), and four overlayer structures (on-top, hcp, and fcc hollow and on bridge), the faulted (hcp) substitutional surface alloy model gives the best experiment-theory agreement. Associated with this structure is a first layer expansion of 4.3%, a second layer contraction of -0.8%, and a third layer expansion of 2.6%. In addition, there is a small amount of buckling of the outermost and third atomic layers as defined in Fig. 1 and Table II. Both the optimum model and the structural parameter values are in full agreement with the recent SXRD study,[12] and in particular support the view that the surface substitutional alloy formed at this surface is displaced to hcp sites to form a stacking fault at the surface alloy/substrate interface. There is now also independent evidence that the same faulted alloy surface phase is produced by Sb adsorption on Cu(111).[12,13]

Prior to these recent studies, there was a growing amount of evidence that Sb occupied substitutional sites at the Ag(111) surface based on *ab initio* calculations,[9] STM,[6,7,11] and CAICISS,[8] but none of these investigations identified the stacking fault. Of course, a key reason for this is that these earlier studies did not consider the possibility of such a stacking fault which, at first sight, appears to be unlikely. It would be of considerable interest to have the benefit of new

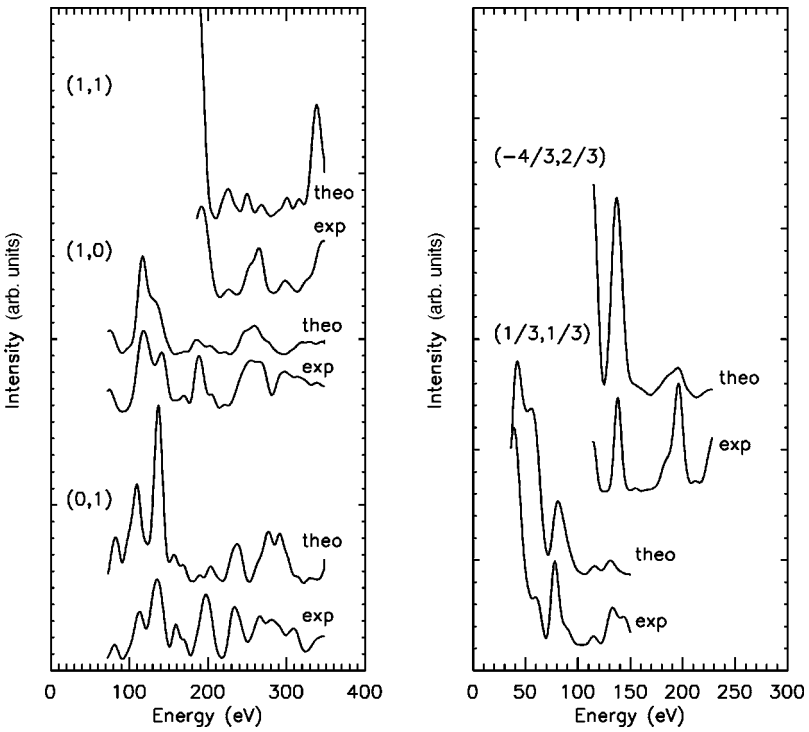

FIG. 3. Comparison of the experimental and best-fit theoretical LEED $I(V)$ curves for the Ag(111)($\sqrt{3}\times\sqrt{3}$)$R30°$-Sb surface. The details of the best-fit faulted substitutional alloy model are given in Fig. 1 and Table II.

ab initio theoretical studies which might cast some light on the underlying driving force for this reconstruction.

ACKNOWLEDGMENTS

The authors are grateful to Professor W. Moritz for supplying the LEEDFIT code and for useful discussions and to Professor M.A. Van Hove and Dr A. Barbieri for supplying the BARBIERI/VAN HOVE PHASE SHIFT and the SATLEED packages. We also would like to thank CNPq, FAPEMIG, and CADCT (Brazilian research agencies) and the European Community (Grant No. CI1*CT940-0063 supporting the Warwick/UFMG collaboration) for financial support.

*Present address: Material Science Division, Lawrence Berkeley National Laboratory, Berkeley, California, 94720. Electronic address: edmar@mailman.lbl.gov

[1] M. Copel, M.C. Reuter, Efthimios Kaxiras, and R.M. Tromp, Phys. Rev. Lett. **63**, 632 (1989).
[2] B. Voigtländer and A. Zinner, Surf. Sci. Lett. **292**, L775 (1993).
[3] M. Copel, M.C. Reuter, M.Horn von Hoegen, and R.M. Tromp, Phys. Rev. B **42**, 11 682 (1990).
[4] M.Horn von Hoegen, M. Pook, A.Al Falou, B.H. Müller, and M. Henzler, Surf. Sci. **24**, 53 (1993).
[5] S. Esch, M. Hohage, T. Michely, and G. Comsa, Phys. Rev. Lett. **72**, 518 (1994).
[6] H.A. van der Vegt, H.M. van Pinxteren, M. Lohmeier, E. Vlieg, and J.M.C. Thornton, Phys. Rev. Lett. **68**, 3335 (1992).
[7] J. Vrijmoeth, H.A. van der Vegt, J.A. Meyer, E. Vlieg, and R.J. Behm, Phys. Rev. Lett. **72**, 3843 (1994).
[8] T.C.Q. Noakes, D.A. Hutt, C.F. McConville, and D.P. Woodruff, Surf. Sci. **372**, 117 (1997).
[9] S. Oppo, V. Fiorentini, and M. Scheffler, Phys. Rev. Lett. **71**, 2437 (1993).
[10] J.A. Meyer, H.A. van der Vegt, J. Vrijmoeth, E. Vlieg, and R.J. Behm, Surf. Sci. **355**, L375 (1996).
[11] H.A. van der Vegt, J. Vrijmoeth, R.J. Behm, and E. Vlieg, Phys. Rev. B **57**, 4127 (1998).
[12] S.A. de Vries, W.J. Huisman, P. Goedtkindt, M.J. Zwanenburg, S.L. Bennett, I.K. Robinson, and E. Vlieg, Surf. Sci. **414**, 159 (1998).
[13] P. Bailey, T.C.Q. Noakes, and D.P. Woodruff, Surf. Sci. **426**, 358 (1999).
[14] I. Meunier, J.-M. Gay, L. Lapena, B. Aufray, H. Oughaddou, E. Landemark, G. Falkenberg, L. Lottermoser, and R.L. Johnson, Surf. Sci. **422**, 42 (1999).
[15] A. Barbieri and M.A. Van Hove (private communication); http://electron.lbl.gov/leedpack/.
[16] G. Kleinle, W. Moritz, D.L. Adams, and G. Ertl, Surf. Sci. Lett. **219**, L637 (1989).
[17] G. Kleinle, W. Moritz, and G. Ertl, Surf. Sci. **238**, 119 (1990).
[18] H. Over, U. Ketterl, W. Moritz, and B. Ertl, Phys. Rev. B **46**, 15 438 (1992).
[19] H. Over, W. Moritz, and G. Ertl, Phys. Rev. Lett. **70**, 315 (1993).
[20] W. Moritz and J. Landskron, Surf. Sci. **337**, 278 (1995).
[21] M.A. Van Hove, W. Moritz, H. Over, P.J. Rous, A. Wander, A. Barbieri, N. Materer, U. Starke, and G.A. Somorjai, Surf. Sci. Rep. **19**, 191 (1993).
[22] N. W. Ashcroft and N. D. Mermin, *Solid State Physics* (HRW International Editions, New York, Holt, Rinehart and Winston, 1976).
[23] E.A. Soares, V.B. Nascimento, V.E. de Carvalho, C.M.C de Castilho, A.V. de Carvalho, R. Toomes, and D.P. Woodruff, Surf. Sci. **419**, 89 (1999).